Transport properties of multi-walled carbon nanotubes based conducting polythiophene / polyaniline nanocomposites

Milind D. Deshpande, Subhash B. Kondawar*

Department of Physics, Polymer Nanotech Laboratory, Rashtrasant Tukadoji Maharaj,
Nagpur University, Nagpur 440033, India

*Corresponding author. Tel: (+91) 7122042086; E-mail: sbkondawar@yahoo.co.in

ABSTRACT

In this paper, we report the influence of functionalized multi-walled carbon nanotubes (MWCNTs) on transport properties of conducting polymers polythiophene (PTH) and polyaniline (PANI). Nanocomposites based on multi-walled carbon nanotubes were synthesized by *in-situ* oxidative polymerization of thiophene/aniline monomer in the presence of functionalized MWCNTs. These nanocomposites have been characterized by SEM, UV-VIS, FTIR, and XRD to study the effect of incorporation of MWCNTs on the morphology, structure and crystalline of the conducting polymers. Nanocomposites have shown high electrical conductivity compared to that of pure PTH/PANI. The enhancement in conductivity of the nanocomposites is due to the charge transfer effect from the quinoid rings of the PTH/PANI to the MWCNT. The effect of MWCNT on the transport properties of PTH and PANI was systematically studied and compared in terms of transport parameters. Charge localization length and most probable hopping distance were found to be decreased with wt % of CNT, whereas the charge hopping energy was found to be increased in nanocomposites. The improved transport properties of both the types of nanocomposites due to incorporation of CNT in conducting polymer matrix can be utilized for solar cells, capacitors, electronic devices as well as chemical sensors. Copyright © 2016 VBRI Press.

Keywords: Conducting polymers; multi-walled carbon nanotubes; polythiophene; polyaniline; nanocomposites.

Introduction

Nanocomposites based on conducting polymers and carbon nanotubes have gained great interest for their unique physical and chemical properties. An interesting application can be the embedding of little quantity of CNTs inside the polymer matrix of conducting polymers for the fabrication of nanocomposites which can be carried out by polymerizing the monomer in the presence of a dispersion of CNTs, is very simple **[1].** In 1977, the discovery of semiconducting and metallic properties of polyacetylene by A.G. MacDiarmid, A. J. Heeger, H. Shirakawa and coworkers **[2, 3]** elicited a tremendous research activity. The conducting polymers were found to be suitable for gas sensor **[4]**, functional hybrid **[5]**, as pH switching electrical conducting biopolymer hybrid for sensor applications **[6]**, as an electrically active redox biomaterial for sensor applications **[7]**. The concept of conducting polymer was then no longer restricted for polyacetylene but extended to all other conjugated hydrocarbon and aromatic heterocyclic polymers such as polyaniline (PANI), polythiophene (PTH), poly (phenylene sulfide) (PPS), polypyrrole (PPY), etc. From molecular structure point of view, a highly delocalized π-conjugation system is found to be possessed by conducting polymers. Upon oxidative doping (oxidation reactions), an electron is removed from the π-system of polymer backbone producing a free radical and a spinless positive charge. The radical and cation are coupled to each other via local resonance of the charge and the radical. The structural distortion site has higher energy level than the rest of polymer chain. This combination of the charged site and paramagnetic defect site is viewed as a polaron, and it creates a new localized energy state in the gap with a single electron occupies the lower energy state. Upon further doping (oxidation), the bipolaron (two separated charged defects) can be produced through either removing free radicals from polarons or recombination of polarons. Upon continuous doping, bipolaron states will gradually form a continuous bipolaron bands. Theoretically, at 100% doping level, the upper and the lower bipolaron bands will merge with the conduction and the valence bands respectively to produce partially filled bands and metallic conductivity **[8].** Conduction by polarons or bipolarons is now generally accepted as the dominant mechanism of interchain transport. Charges on the polymer backbone must hop from chain to chain, as well as move along the chain, for bulk conductivity to be possible.

After the report of preparation of carbon nanotubes (CNTs) based conducting polymer nanocomposites, there have been efforts to combine carbon nanotubes and different conducting polymers such as polyacetylene, polypyrrole, polythiophene, polyaniline etc. to produce advanced functional composite materials with desirable electrical, optical and mechanical properties **[9].** Since the discovery by Iijima **[10],** carbon nanotubes (CNTs) have

received much attention for their possible use in fabricating new classes of advanced materials, due to their unique structural, optical, mechanical and electronic properties [**11-13**]. Addition of CNTs in the matrix of conducting polymers changes their behavior mostly towards the electrical conductivity [**14-17**]. Due to conducting polymer-CNT networks, these materials are of great interest for electronic applications including photovoltaic cells, organic light emitting diodes, electromagnetic shielding, electro static dissipation, antennas, and batteries [**18**]. To the best of our knowledge, there is a lot of research work reported on the preparation of conducting polymer-CNT composites to improve the electrical conductivity of the host polymer, but no one has reported the change in transport parameters of the composites. Rajalakshmi *et al.* [**19**] reported functionalized multi-walled carbon nanotubes-nanostructured conducting polymer composite modified electrode for the sensitive determination of uricase inhibitor. Recently, Gao *et al.* [**20**] reported conducting polymer/carbon particle thermoelectric composites: emerging green energy materials. Pang et al [**21**] reported dynamic high potential treatment with dilute acids for lifting the capacitive performance of carbon nanotube/conducting polymer electrodes. Chehata *et al.* [**22**] reported Optical and electrical properties of conducting polymer-functionalized carbon nanotubes nanocomposites. Zhou *et al.* [**23**] reported the strong interaction in conjugated systems greatly improves the charge transfer reaction between polyaniline and the carbon nanotube prepared by an in-situ polymerization of aniline monomers using multi-walled carbon nanotubes with minimized defects as templates. Mahore *et al.* [**24**] reported carbon nanotube/polyaniline based ternary nanocomposites as electrode materials for supercapacitors. Similarly, thiophene-based conducting polymers have attracted considerable attention during the past two decades due to a wide range of unique optical, electrochemical and electronic applications. Especially low band gap thiophene-based polymers are very promising materials with high conductivities, high degrees of optical transparency, and enhanced nonlinear response. Polythiophene based polymers are currently applied in many fields such as polymeric light-emitting diodes, conducting polymer-based actuators, supercapacitor, corrosion protection, antistatic coatings, transparent electrodes for inorganic electroluminescent devices, sensors, rechargeable batteries, electrochromic windows, and photovoltaic devices, etc. [**25**]. Wang *et al.* [**26**] and Du *et al.* [**27**] studied the thermoelectric properties of polythiophene/multiwalled carbon nanotube composites. Electrochemical and Raman spectro-electrochemical investigation of single-wall carbon nanotubes–polythiophene hybrid materials was studied by Pokrop *et al.* [**28**]. Solid state heating method was used to study electrochemical properties of the poly(3,4-ethylenedioxythiophene)/single-walled carbon nanotubes composite [**29**]. Due to van-der Waals forces, tight bonding of CNT limits their applications. Cynthia Oueiny and co-workers worked on the applications of electrochemically synthesized PANI/CNTs nanaocomposites [**30**], but in none of the reported works MWCNTs were functionalized before incorporating into polymer matrix. In this paper we report the influence of functionalized multi-walled carbon nanotubes (MWCNTs) on transport properties of

conducting polymers polythiophene (PTH) and polyaniline (PANI). This work describes the synthesis and characterization of protonic acid doped PANI and PTH functionalized MWCNT fabricated by an in-situ chemical oxidative polymerization method. The detailed electrical transport properties [**31**] of PANI/CNT and PTH/CNT composites, in the form of the transport parameters such as dc electrical conductivity (σ), charge localization length (α^{-1}), most probable hopping distance (R) and charge hopping energy (w) are reported.

Experimental

Chemicals

Aniline, Thiophene (99%) (Merck) were purified by distillation under reduced pressure. The oxidant, Ammonium per sulphate (APS), ferric chloride ($FeCl_3$, Merck) was used in preparation of PANI and PTH respectively. Double distilled water was prepared and used as solvent in preparation of PANI whereas Chloroform ($CHCl_3$, Merck) was used in preparation of PTH. Methanol (CH_3OH, Merck) was also used to remove residual impurities from PTH. High purity MWCNTS of diameter 30 - 40 nm was made available from NPL, New Delhi, India. Other supplement chemicals were of AR grade and used as received.

Functionalization of MWCNTs

Due to van-der Waals forces, tight bonding of CNT limits their applications. Therefore, in this study MWCNTs surface is functionally modified by ultrasonication using H_2SO_4 and HNO_3 to provide specificity for improved interaction between CNT and polymer matrix which enhances the processability and properties of composites. The solution of 6M H_2SO_4 and 6M HNO_3 in 3:1 ratio was stirred for 10 minute. MWCNTs were added to it and then solution was sonicated for 4 hours at 50^oC. After centrifugation MWCNTs was filtered, washed and dried to get functionalized MWCNTs (f-MWCNTs).

Synthesis of PANI-MWCNT and PTH-MWCNT nanocomposites

The synthesis of PANI-MWCNT nanocomposites was performed using in-situ oxidative polymerization of aniline in presence of 5% and 10% of functionalized MWCNT in 1 M HCl using ammonium persulphate as an oxidant. The pure conducting polymer (PANI) was also synthesized by following the same steps carried out for the nanocomposites without MWCNT. The synthesis of PTH-MWCNT nanocomposites was performed using in-situ oxidative polymerization of thiophene mixed in chloroform in presence of 5% and 10% of functionalized MWCNT in 1 M HCl using anhydrous ferric chloride as an oxidant. The pure conducting polymer (PTH) was also synthesized by following the same steps carried out for the nanocomposites without MWCNT.

Characterizations

Fourier transform infrared (FTIR) spectra were recorded in the range 600-4000 cm^{-1} with 4 cm^{-1} resolutions. UV-vis spectra were recorded in the range 200-800 nm on UV-1800 Shimatzu. Rigaku Mini Flex-II a bench top X-ray

Diffraction instrument was used to study XRD patterns. Sample morphology was studied by scanning electron microscopy (SEM) using JEOL JSM-6360 analytical scanning electron microscope. Direct current (dc) electrical conductivity of the polymers and their composites were measured using standard four probe instrument and the pellets were prepared with the help of hydraulic press (Kimaya Engineers, India) by applying a pressure of 5000 kg/cm^2. Impedance analysis is done using Wayn kerr impedance precision analyzer (6500 B).

Results and discussion

FTIR spectroscopy

FTIR spectra of PANI and PANI-CNTs composites and that of PTH and PTH-CNTs composites are shown in **Fig. 1(a, b)** respectively. The spectra of PANI show the characteristic vibration bands at the vicinity of 3395, 1545, 1513, 1307and 1141 cm^{-1}. A band at 3394.51 cm^{-1} assigned to N-H stretching vibration. The ring stretching of quinoid (N=Q=N) and benzenoid (N-B-N) form was observed at 1544.81 and 1512.79 cm^{-1} respectively for PANI indicating the oxidation state of emaraldine salt of PANI. C-N stretching band of an aromatic amine appears at 1306.55cm^{-1}. All these bands are well matched with the previously reported values for polyaniline prepared using hydrochloric acid **[32]**. The intensity of the C-N stretching band appearing at 1306.55cm^{-1} indicates the long length of PANI. The change in the intensity of these bands can be observed due to addition of fillers, type of dopant and the conditions at the time of polymerization. The strong band around 1141 cm^{-1} is the characteristic peak of PANI conductivity and is a measure of the degree of the delocalization of electrons **[33]**. The peak at 802 cm^{-1} represents the C-H out of plane bending. Increase in the intensity peaks around 1545, 1513 cm^{-1} confirms the addition of CNTs. The intensity of peaks found to be reduced considerably for PANI-5% CNTs composition which suggests the stability of Quinoid and Benzenoid bands in this composition. It is found that as the weight % of CNTs increases, the peak related to C-N stretching reduces which indicate the enhancement in the chain length of the composite as compare to pure PANI which may be the reason for the variation in room temperature conductivity for the PANI/CNTs nanaocomposites.

The spectra of PTH consist of a band at 3392 cm^{-1} is assigned to C-H aromatic stretching and 2930 cm^{-1} assigned to C-H aliphatic stretching. The strong band around 1690 cm^{-1} is the characteristic peak of PTH conductivity and is a measure of the degree of the delocalization of electrons. The aromatic nuclei stretching of C=C was observed at 1545 and 1512 cm^{-1} respectively for PTH. At 1101 cm^{-1} there observe an in-plane C–H aromatic bending vibrations of substituted thiophene ring are situated. Peak at 1013 cm^{-1} assigned to C=S stretching and a tiny peak at 853 cm^{-1} assigned to C-S stretching. The strong intensity of the 790 cm^{-1} band, is assigned to C-H bending which is characteristic of 2,5-disubstituted thiophene rings, indicates that chemical coupling of thiophene rings occurs preferentially at the 2,5-positions. The peaks at 1690, 1013, 853 and 790 cm^{-1} confirm the synthesized material is polythiophene. All these bands are well matches with the

previously reported values for polythiophene prepared using Ferric Chloride and Chloroform. The slight shifting and change in intensity in the peak at 3392 cm^{-1} is observed due to addition of CNTs. The characteristic peaks of PTH at 1013 and 783 cm^{-1}first get suppressed for lower weight percentage of PTH and gradually increases in intensity also get broadened while C-S stretching peak disappears with increase in weight percentage of CNTs. This suggests a strong interaction of added CNTs with PTH and stable C-S bonds. Along with these bands increase in the intensity peaks around 1545, 1513 cm^{-1} confirms the addition of CNTs as it is related to C=C stretching. The vibration peaks reduce for nanocomposites confirms the increase in the length of polymeric chain.
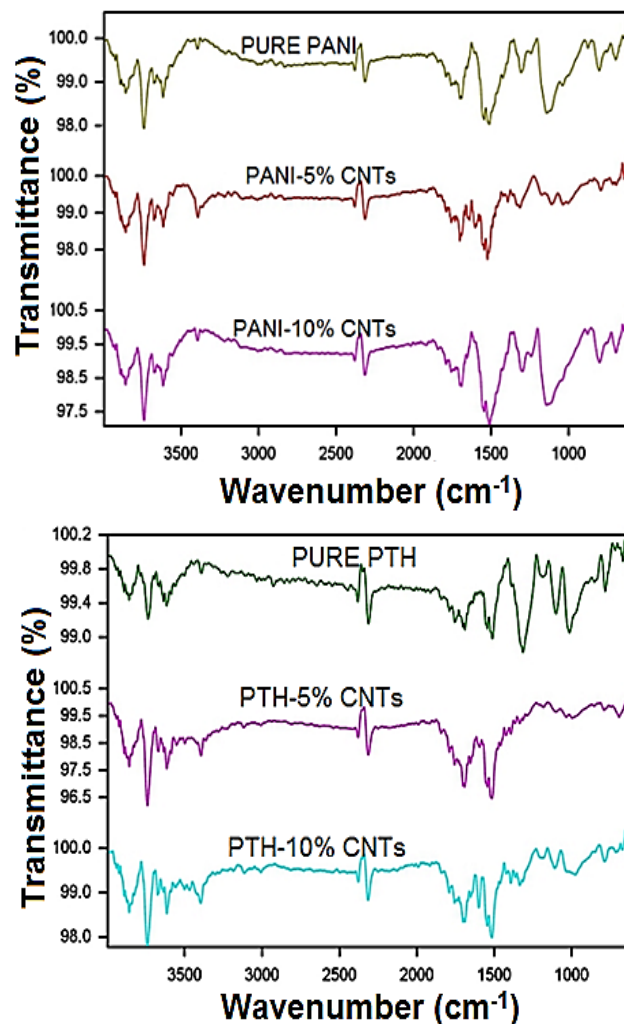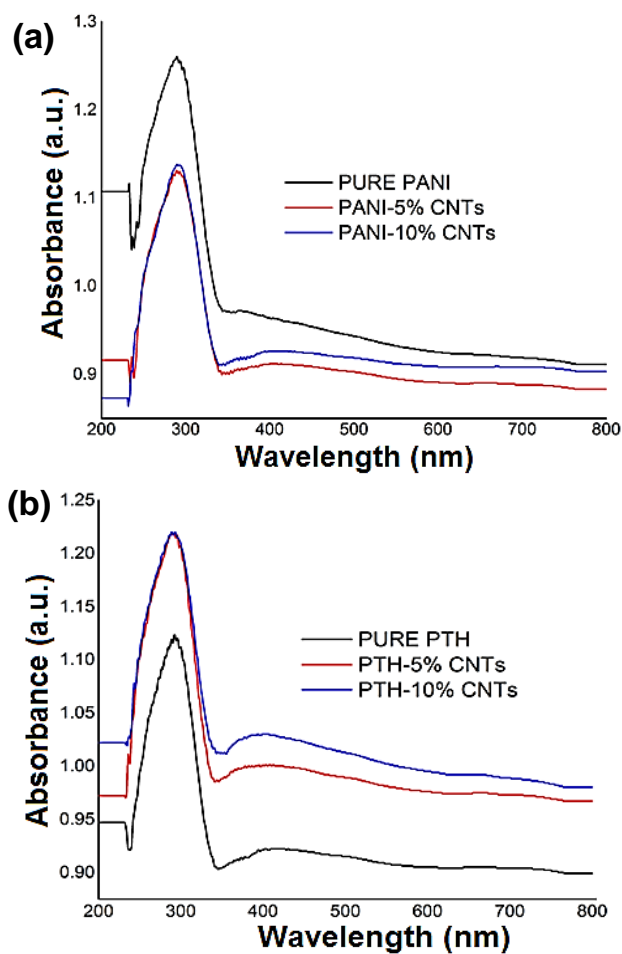

Fig. 1. (a) FTIR spectra of PANI and PANI-CNTs composites and (b) FTIR spectra of PTH and PTH-CNTs composite.

UV-vis spectroscopy

UV-vis spectra of PANI and PANI-CNTs composites and that of PTH and PTH-CNTs composites are shown in **Fig. 2(a, b)** respectively. In case of pure PANI, two absorption maxima, one in the UV region and other in the visible region are observed. The fine structured absorption bands in the range 235-340 nm is associated with $\pi \rightarrow \pi^*$ transitions, as it is theoretically predicted and later on experimentally proved in polyaniline and its derivatives

and a broad band around 350-615 nm is due to $n \rightarrow \pi^{\bullet}$ of an excitation band which is interring charge transfer associated with the excitation from benzenoid to quinoid moieties **[34].** The observed peaks thus confirm that prepared PANI is in conducting form. UV-vis spectra of PANI/CNTs nanocomposites illustrates that the composites also show two absorption bands. The band in the UV region is slightly shifted to lower wavelength side so the wavelength spread is increased due to addition of CNTs. But at the same time slope of band seems to shift towards higher wavelength side which might result in increased conductivity of nanocomposites over PANI.

Fig. 2. (a) UV-Vis spectra of PANI and PANI-CNTs composites and (b) UV-Vis spectra of PTH and PTH-CNTs composites.

The λ_{max} peak found shifting towards higher wavelength with increase in the weight % of CNTs in the PANI matrix. For 10% of CNTs the peaks found shifted at 289.94 nm. Also the change is observed in the visible band which shows the shift in wavelength towards shorter side similar to the UV band. Also the highest wavelength of this band found shifting of towards higher. The 363.71 nm peak found shifted up to 413.73nm for 10% CNT composite. The blue shift of the bands is a result of incorporation of CNTs in the PANI matrix. In the PANI/CNTs nanocomposites as compare to PANI shifting of λ_{max} toward lower wavelength indicates the formation of nanomaterials and spreading of band indicates the formation of more number of polarons and bipolarons which has been confirmed from the enhanced electrical conductivity for these composites. In

case of pure PTH, there also observes two absorption maxima, one in the UV region and other in the visible region similar to the PANI. The fine structured absorption bands in the range 237-340 nm is associated with $\pi \rightarrow \pi^{\bullet}$ transitions, as per the theoretical prediction **[35]** experimental results also show a broad band around 350-590 nm is due to $n \rightarrow \pi^{\bullet}$ of an excitation band which is interring charge transfer associated with the polaronic/bipolaronic charge transfer.

The absorption by compounds containing extended conjugated systems are caused by transitions that arises from delocalized π electrons system. In composites of PTH/CNTs the band in the UV region is slightly shifted to lower wavelength side so the wavelength spread is increasing due to addition of nano fillers CNTs. But at the same time λ max seem to shift towards higher wavelength side which results in to increase in the conductivity of nanocomposites over PTH. The λ_{max} peak found shifting towards higher wavelength with increase in the weight % of CNTs in the PTH matrix.

For 10% of CNTs the peaks found shifted at 292.28 nm. In addition to this the highest wavelength of this band found shifting of towards lower wavelength. The 418.92 nm peak found shifted up to 393.32 nm for 10% CNT composite. The blue shift of the bands is a result of incorporation of CNTs in the PTH matrix. The enhanced absorption of PTH/CNTs nanocomposites as compare to PTH indicates the formation of more number of polarons and bipolarons which has been confirmed from the enhanced electrical conductivity for these composites.
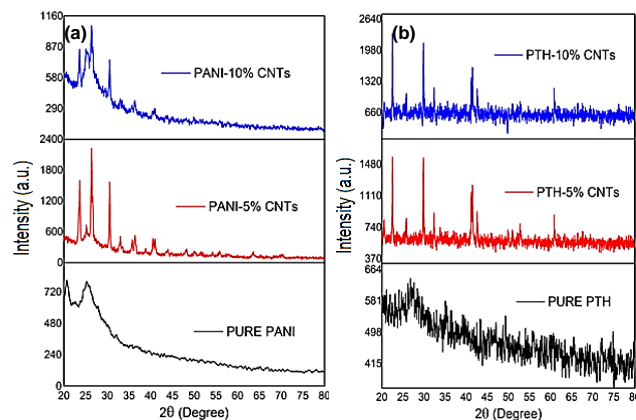
Fig. 3. (a) XRD pattern of PANI and PANI-CNTs composites and **(b)** XRD pattern of PTH and PTH-CNTs composites.

X-ray diffraction

XRD patterns of PANI and PANI/CNT composites and that of PTH and PTH/CNT composites are shown in **Fig. 3(a)** and **(b)** respectively. When carbon nanotubes were incorporated into the PANI matrix, the sharp and strong diffraction peak of CNT at (26.28°) was overlap with the peak of PANI which results in the broad and intense peak in the composite results in homogeneous coating of PANI onto the CNTs indicating that CNTs were well dispersed in polymer matrix **[36, 37]**. Also two intense peaks one at 26.71° and other at 30.6° are observed in PANI composites suggest the more crystalline structure of PANI composites. When XRD patterns of conducting PTH and its nanocomposites as shown in figure 3(b) are taken into

consideration, PTH peak is observed at 25.90° which seems enhanced due to incorporation CNTs in the PTH composites. Intense peaks at 22.6, 29.77, 32.16, 41.42 and 60.83° confirms the more crystalline structure of PTH composites. Intensity of all the peaks in PTH seems to increase in its composites. This result shows that the homogeneous coating of PTH onto the CNTs indicating that CNTs were well dispersed in polymer matrix [38] as seen from SEM also.

SEM micrographs

SEM images of MWCNTs, functionalized MWCNTs and PANI-CNT and PTH-CNT composite are shown in **Fig. 4**. Composite shows the homogeneous coating of polymers onto the CNT indicating that carbon nanotubes were well dispersed in polymer matrix. Rough surface and increased diameter of the composite indicated the coating of polymer over the CNTs since diameter of CNTs was 30-40 nm. Nanocomposites show successful coating of polymers on CNTs which gives conductive pathway and leads to high conductivity as compared to that of pure polymer (PANI & PTH). The multilayer structure of polymer nanocomposites of PANI and PTH seem porous. This porous structure may be helping in storage of charge and hence capacitive property of PTH increased by adding MWCNTs.
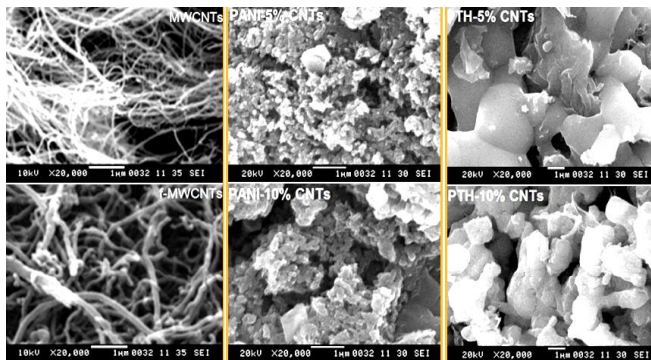
Fig. 4. SEM micrographs of MWCNTs, f-MWCNTs, PANI-5% CNTs, PANI-10% CNTs, PTH-5% CNTs and PTH-10% CNTs.

Electrical conductivity and transport properties

Fig. 5(a) and **(b)** shows the variation in electrical conductivity of PANI, its composites and PTH, its composites with temperature respectively. Increase in room temperature conductivity of PANI is observed due to addition of functionalized MWCNTs. The conductivity of 5.24 S/cm at 303 K is observed for Pure conducting PANI which enhances to 6.72 S/cm by addition of functionalized MWCNTs 10% with respect to aniline monomer and increases with increase in temperature, confirms the semiconducting nature of PANI and its nanocomposites. Similarly PTH and its composites also show semiconducting nature. Pure conducting PTH shows room temperature conductivity 1.14×10^{-4} S/cm which enhances drastically to 4.05×10^{-2} S/cm by addition of functionalized MWCNTs 10% with respect to thiophene monomer.

The variation of conductivity of polymer nanocomposites with temperature indicate the "thermal activated" behavior as that of pure polymers. Polymer-CNT interaction could

facilitate the charge transfer process between them and influence the charge transport properties of composite. The room temperature conductivity of the nanocomposite along with transport parameters are reported in **Table 1**.
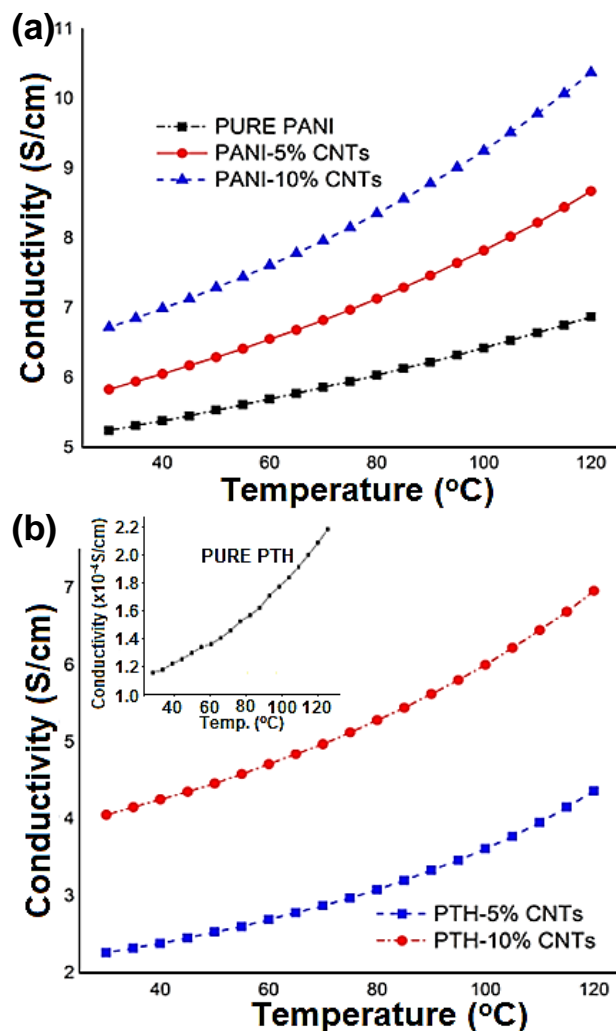

Fig. 5 (a) Conductivity of PANI and PANI-CNTs composites (b) Conductivity of PTH and PTH-CNTs composites

To find transport parameters of the polymer nanocomposites from the data of electrical conductivity, Ziller equation (1) has been used, which describes the interchain conductivity where only the neighbour variable range hoping (VRH) of charge is considered.

$$\sigma(T) = \sigma(o).e^{\left(\frac{T_o}{T}\right)^{1/2}} \tag{1}$$

The plot of $log(\sigma)$ versus $T^{-1/2}$ was found to be linear, hence the characteristic temperature (T_o) was determined from the slope of the line from the plot of $log(\sigma)$ versus $T^{-1/2}$ and then the transport parameters such as charge localization length (α^{-1}), most probable hopping distance (R) and charge hopping energy (w) have been determined using the relations (2), (3) and (4). In these relations, Z is the number of nearest neighbouring chains (~4), k is Boltzmann constant and $N(E_F)$ is the density of states per electron volt. $N(E_F)$ is 1.6 for PANI wherein 0.23 for PTH. MWCNT may serve as 'conducting bridge' connecting the

polymers' conducting domain. Thus functionalized MWCNT embedded in the polymer matrix have better conductivity with enhanced solubility and processability as compared to that of pure conducting polymers.

$$T_o = \left(\frac{8\alpha}{N(E_F)Zk} \right) \tag{2}$$

$$R = \left(\frac{T_o}{T} \right)^{\frac{1}{2}} \left(\frac{\alpha^{-1}}{4} \right) \tag{3}$$
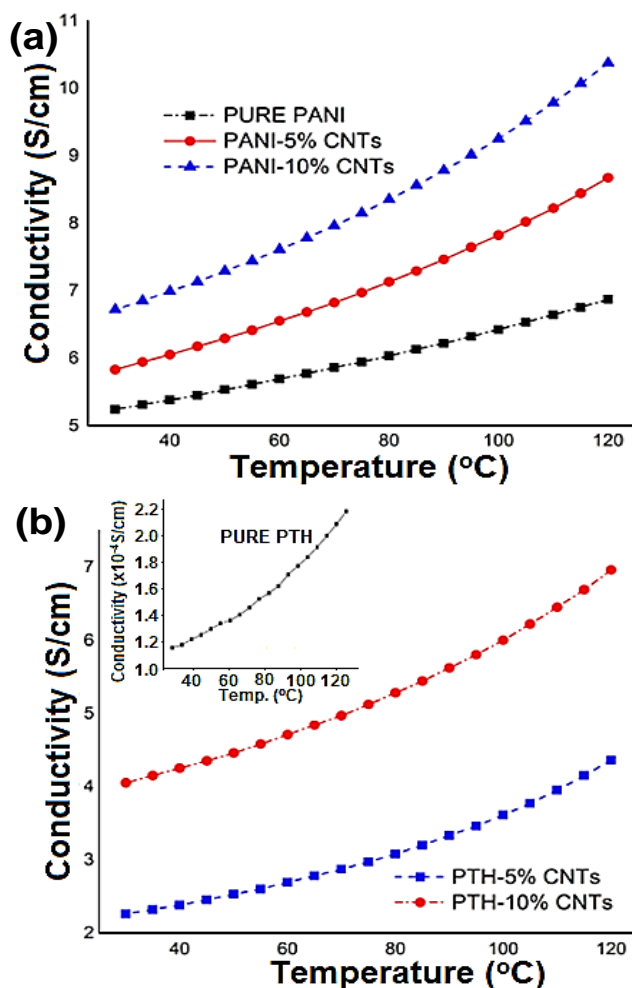
$$w = Zk \frac{T_o}{16} \tag{4}$$

Fig.5. (a, b). Conductivity of PANI and PANI-CNT composites.

Table 1. Transport parameters of Polymers and nanocomposites.

Polymer	σ(S/cm) at 303K	T_o (K)	α^{-1} (nm)	R (nm)	w (eV)
PANI	5.2	1483	6.1	10.7	0.03
PANI-5%CNT	5.8	3162	2.8	7.3	0.06
PANI-10%CNT	6.7	3797	2.3	6.7	0.08
PTH	1.1×10^{-4}	7502	8.3	33.1	0.16
PTH-5%CNT	2.2×10^{-2}	9554	6.5	29.4	0.20
PTH-10%CNT	4.0×10^{-2}	12098	5.3	21.7	0.39

Conclusion

Functionalized MWCNTs were successfully incorporated in PANI and PTH matrix using in-situ oxidative polymerization. FTIR spectra confirm the interaction of MWCNTs with polymers. Variation in λ_{max} due to addition of MWCNTs was observed in UV-VIS spectra. XRD confirms the unification of MWNCTs with polymers which gives more crystalline structure of polymer nanocomposites. SEM images of composites show the homogeneous coating of polymers onto the MWCNTs indicating that carbon nanotubes were well dispersed in polymer matrix. The drastic variation in conductivity due to addition of MWCNTs in the polymer matrix is observed. It is found that as the wt. % of CNTs increases in polymer, conductivity of the composite increases promptly. The general study of impedance shows the synthesized PANI and its composites are better for preparation of inductors/resistors and hence nanocomposites of PANI can be used in making electronic devices, chemical sensors. On the other hand, PTH and its composites are better for preparation of capacitors and hence nanocomposites of PTH can be utilized in solar cells and fuel cells.
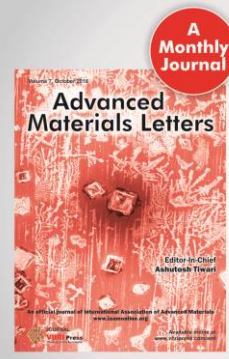
References

1. Bavastrello, V.; Terencio, T. B. C.; Nicolini, C; *Polymer*, **2011**, *52*,46.
   DOI: 10.1016/j.polymer.2010.10.022
2. Heeger, A; *J. Phys. Chem. B.*, **2001**, 105(*36*), 8475.
   DOI: 10.1021/jp011611w
3. MacDiarmid, A; *Angew. Chem. Int. Ed.*, **2001**, *40*, 2581.
   DOI: 10.1002/1521-3773(20010716)40:14<2581::AID ANIE2581>3.0.CO;2-2
4. Tiwari, A.; Kumar, R.; Prabhakaran, M.; Pandey, R.R.; Kumari, P.; Chadurvedi, A.; Mishra, A.K; *Polymers for Advanced Technologies,* **2010**, *21*, 615.
   DOI: 10.1002/pat.1470
5. Tiwari, A.; Sen, V.; Dhakate, S.R.; Mishra, A.P; Singh, V; *Polymers for Advanced Technologies,* **2008**, *19*, 909.
   DOI: 10. 1002/pat.1058
6. Tiwari, A; *Journal of Polymer Research*, **2008**, 15(4), 337.
   DOI: 10.1007/s10965-008-9176-4
7. Tiwari, A; *Journal of Macromolecular Science, Part A: Pure and Applied Chemistry,* **2007**, 44(7), 735.
   DOI: 10.1080/10601320701353116
8. Lu, M.; Yang, S; *Synth. Met.,* **2005**, *154*, 73.
   DOI: 10.1016/j.synthmet.2005.07.014
9. Chakraborty, G.; Ghatak, S.; Meikap, A.; Woods, T.; Babu, R.; Blau, W; *Journal of Polymer Science: Part B: Polymer Physics,* **2010**, *48*, 1767.
   DOI: 10.1002/polb.22042
10. Iijima, S; *Nature,* **1991**, *354*, 56.
    DOI: 10.1038/354056a0
11. Amente, C.; K. Dharamvir; *J. Nanosci. Engg.,* **2015**, *5*, 17.
    DOI: 10.4236/wjnse.2015.51003
12. Odom, T.W.; Huang, J.L.; Kim, P.; Lieber, C; *Nature,* **1998**, *391*, 62.
    DOI: 1998;391:62–4
13. Santos, C.; Hernandez, A.L.M.; Fisher, F; *Chem. Mater.,* **2003**, *15*, 4470.
    DOI: 2003;15(23):4470–5
14. Zhong, H.; Yuan, R.; Chai, Y.; Li, W.; Zhong, X; *Talanta,* **2011**, *85*, 104.
    DOI: 10.1016/j.talanta.2011.03.040
15. Kondawar, S.; Anwane, S.; Nandanwar, D.; Dhakate, S. *Adv. Mat. Lett.* **2013**, *4(1),* 35
    DOI: 10.5185/amlett.2013.icnano.101
16. Kondawar, S.; Deshpande, M.; Agrawal, S. *International Journal of Composite Materials,* **2012**, 2(3): 32
    DOI: 10.5923/j.cmaterials.20120203.03
17. Sharma, A.; Sharma, Y.; Malhotra, M.; Sharma, J. *Adv. Mat. Lett.* **2012,** *3(2),* 82

DOI: 10.5185/amlett.2012.1315

18. Woo, H.; Czerw, R.; Webster, S.; Carroll, D. *Synthetic Metals,* **2001**, 116*(1)*, 369
DOI: 10.1016/S0379-6779(00)00439-2

19. Rajalakshmi, K..; John, S. A.; *Electrochimica Acta***, 2015**, *173*, 506
DOI: 10.1016/j.electacta.2015.05.101

20. Gao, C.; Chen, G.; *Comp. Sci. Tech.*, **2016**, *124*, 52
DOI: 10.1016/j.compscitech.2016.01.014

21. Pang, Q. Y.; Yung, K. C.; *J. Electroanal. Chem.*, **2015**, *758*, 125
DOI: 10.1016/j.jelechem.2015.10.022

22. Chehata, N.; Ltaief, A.; Bkakri, R.; Bouazizi**,** A.; *Mater. Sci. Semicond. Proc.***, 2014,** *22*, 7
DOI: 10.1016/j.mssp.2014.02.010

23. Zhou, Y.; Qin, Z. Y.; Li, L.; Zhang, Y.; Wei, Y. L.; Wang, L. F.; Zhu, M. F; *Electrochimica Acta*, **2010**, *55*, 3904
DOI: 10.1016/j.electacta.2010.02.022

24. Mahore, R.; Kondawar, S.; Burghate, D.; Meshram, B; *Journal of the Chinese Advanced Materials Society,* **2015**, 3*(1)*, 45
DOI: 10.1080/22243682.2014.956337

25. Lv, R.; Sun, Y.; Yu, F.; Zhang, H; *Journal of Applied Polymer Science,* **2011***,* 124*(1),* 855
DOI: 10.1002/app.35117

26. Wang, L.; Jia, X.; Wang, D.; Zhu, G.; Li; *J. Synthetic Metals*, **2013**, *181*, 79
DOI: 10.1016/j.synthmet.2013.08.011

27. Du, Y.; Shen, S. Z.; Yang, W. D.; Cai, K. F.; Casey, P; *Synthetic Metals*, **2012,** 162 *(3–4)*, 375
DOI: 10.1016/j.synthmet.2011.12.023

28. Pokrop, R.; Kulszewicz-Bajer, I.; Wielgus, I.; Zagorska, M.; Albertini, D.; Lefrant, S.; Louarn, G.; Adam Pron, A; *Synthetic Metals*, **2009,** 159 *(9)*, 919
DOI: 10.1016/j.synthmet.2009.01.056

29. Abdiryim, T.; Ubul, A.; Jamal, R.; Xu, F.; Adalet Rahman, A; *Synthetic Metals*, **2012**, *162*, 17
DOI: 10.1016/j.synthmet.2012.07.007

30. Cynthia, O.; Sophie, B; François-Xavier, P; *Progress in Polymer Science,* **2014**, 39*(4)*, 707.
DOI: 10.1016/0379-6779(91)91110-V

31. Kondawar, S.; Hedau, M.; Tabhane, V.; Dongare, S.; Mahatme, U.; Mondal, R; *Modern Phy. Lett. B,* **2006,** *20(23),* 1464.
DOI: 10.1142/S0217984906011517

32. Quillard, S.; Louarn, G.; Lefrant, S.; MacDiarmid, A; *Phy. Rev. B*, **1994**, *50*, 12496.
DOI: 10.1103/PhysRevB.50.12496

33. Xia, H.; Wang, Q; *J. Appl. Polym. Sci.*, **2003**, *87*, 1811.
DOI: 10.1007/s10853-006-1120-6

34. Havinga, E.; Rotte, I.; Meijer, E.; Hoeve, W.; Wynberg, H; *Synthetic Metals*, **1991**, 41*(1-2)*, 473.
DOI: 10.1016/0379-6779(91)91110-V

35. Philips, S.; Yu, G.; Heeger, A; *Phys. Rev. B*, **1989**, *39*, 10702.
DOI: 10.1103/PhysRevB.39.10702

36. Zhang, Z.; Wan,M.; Wei, Y; *Adv. Funct. Mater.,* **2006**, *16*, 1100.
DOI: 10.1002/adfm.200500636

37. Dufour,B; Rannou, P.; Fedorko, P.; Djurado, D.; Travers, J.; Pron, A; *Chem. Mat,* **2001**, *13*, 4032.
DOI: 10.1021/cm001224j

38. Manjunath, B.; Venkatraman, A.; Stephen, T. *J. Appl. Polym. Sci.* **2003**, 17*(4)*, 1091.
DOI: 10.1002/app.1973.070170407